

Numerical Simulation of Cold Rolled Steel Sheet Metal during Blanking Process

Peter Pecháč, Milan Sága, Milan Sapieta

Faculty of Mechanical Engineering, Univerzity of Zilina. Unierzitna 1, 010 26 Zilina. Slovak Republic. E-mail: milan.sapieta@fstroj.uniza.sk, peter.pechac@fstroj.uniza.sk, milan.saga@fstroj.uniza.sk

This paper presents numerical simulation of blanking process using finite element method and comparison of results obtained by analytical solution commonly used in engineering practice. The problem was modeled using axial symmetry. Experimental measurement was used to create multi-linear plastic material model. Results of numerical simulation were used to create history of blanking force vs. tool displacement.

Keywords: Blanking process, numerical, sheet metal

1 Introduction

Blanking is the most widely used forming operation. It is used both for the preparation of semi-finished products and cutting of metal parts either for final use or as preparation for other technological operations [1]. Simple analytical calculations are usually used during preparation of serial manufacturing [2]. These analytical calculations are sufficient for determining basic parameters of blanking process as maximal blanking force, however when problems occur during the manufacturing process the solution is often complicated and can be calculated only by using advanced numerical methods [3]. This paper presents a numerical simulation of blanking process for a steel washer using finite element method and compares results of analytic solution with results obtained by finite element method using two different material models.

2 Material data and models

Material data are one of the most important inputs in numerical simulation. Precise results can be obtained only when precise material data in combination with proper material model are used [4,-7].

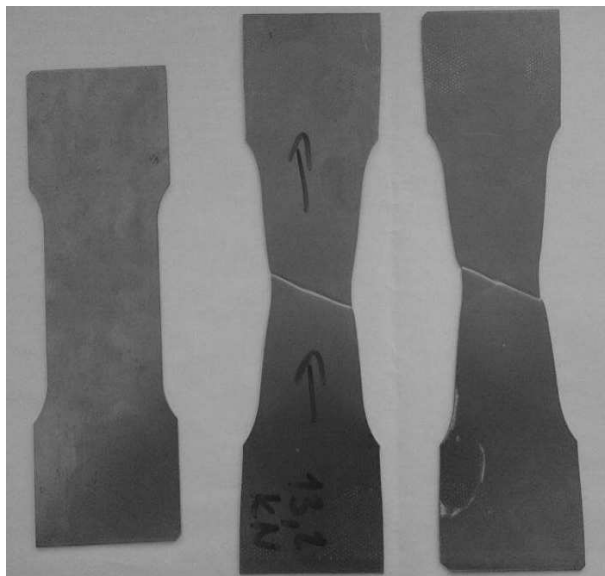


Fig. 1 Specimens for tensile test: specimen before test (left), specimens after rupture (middle and right)

Structural steel S235J was used. Material data used for the presented simulations were obtained by tensile test using sheet metal samples of 1 mm thickness. The shape of the samples before and after tensile test can be seen on the following figure.

3 Analytical calculation of blanking force

Blanking force can be calculated analytically using formula which takes into account ultimate shear strength t_s and shear plane area. This formula is often used in engineering practice [8-12].

The dimensions of the punched ring were: $D_1 = 15.5$ mm, $D_2 = 20.55$ mm. the metal sheet had thickness $t = 2$ mm, and the ultimate strength determined by tensile test was $R_m = 337$ MPa (engineering stress).

The shear plane area is calculated from shear circumference and sheet metal thickness.

Shear circumferences are calculated as follows:

$$s_1 = \pi \cdot D_1, \quad (1)$$

$$s_2 = \pi \cdot D_2, \quad (2)$$

Ultimate shear strength is calculated as follows:

$$t_s = 0.8 \cdot R_m = 269.6 \text{ MPa} \quad (3)$$

Blanking forces for the two shear areas are calculated as follows:

$$F_1 = s_1 \cdot t \cdot t_s = 26256 \text{ N} \quad (4)$$

$$F_2 = s_2 \cdot t \cdot t_s = 34811 \text{ N} \quad (5)$$

The overall blanking force is the sum of forces F_1 and F_2 :

$$F = F_1 + F_2 = 61067 \text{ N} \quad (6)$$

4 FEM model

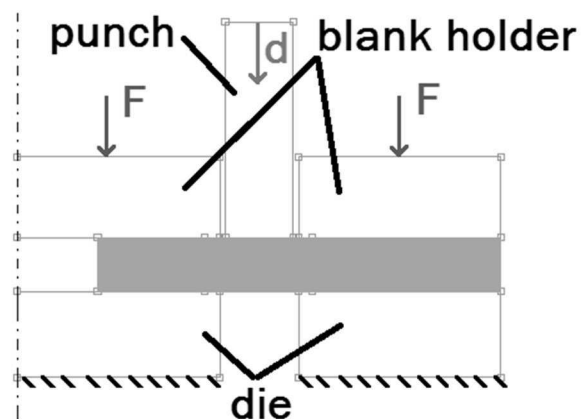


Fig. 2 Tool configuration and boundary conditions

The problem was modeled using axial symmetry in commercial FEM software ADINA. The punch, blank holders and die were modeled as rigid bodies. Rigid target contact was used for contact of punch blank holders and die with sheet metal. Friction coefficient of 0.2 was used for all contacts. The sheet metal was meshed using 2D 4 node elements, with very fine mesh in the area near punch.

In the first the sheet metal was pressed by blank holders using force of 62400 N. The second stage involved displacement of punch, which was prescribed by time function. The punch moved 5 mm downward and then 6 mm upward.

The FEM model with boundary conditions can be seen on following figure:

Detail of FEM mesh can be seen on the following figure:

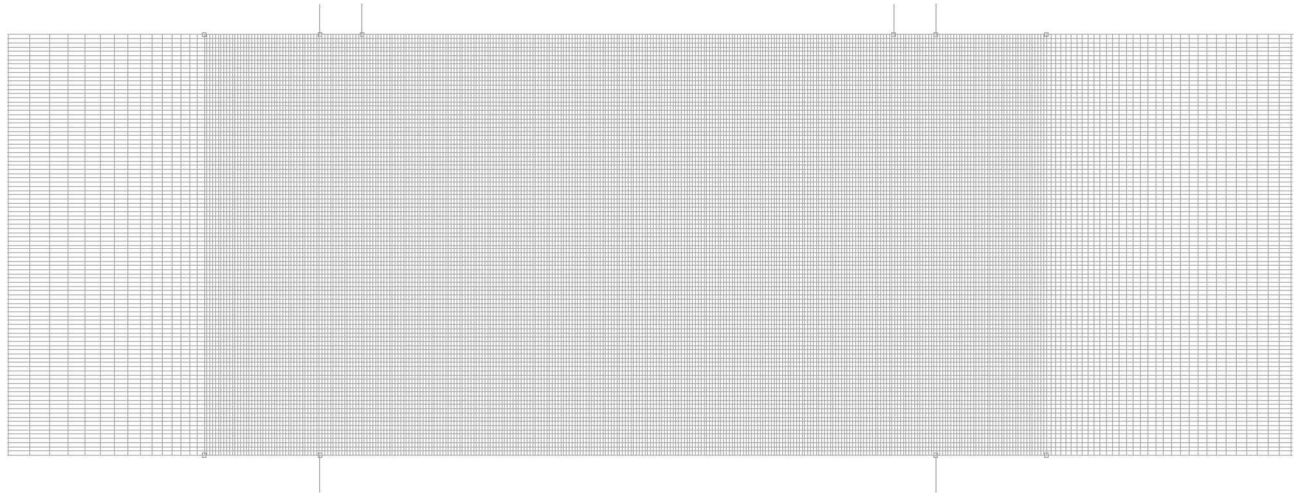


Fig. 3 Detail of finite element mesh in the area subjected to cracking

5 FEM simulation using bilinear material model

The data obtained from tensile test were used to create bilinear elastic-plastic material. Young's modulus $E = 210000$ MPa, Poisson's number $\mu = 0.3$, initial yield stress = 201.918 MPa, strain hardening modulus = 897. Rupture of elements occurred when accumulated effective plastic strain in element reached 0.2731. The material model in true stress representation can be seen on the figure 4.

The accumulated effective strain distribution immediately after the material fully cracked can be seen on the following figure.

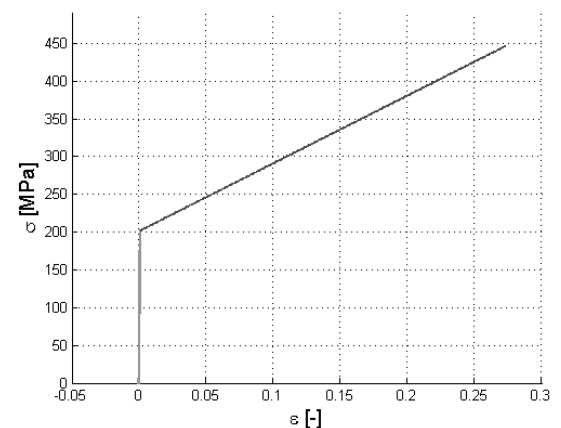


Fig. 4 Stress-strain curve for bilinear material model in true stress representation

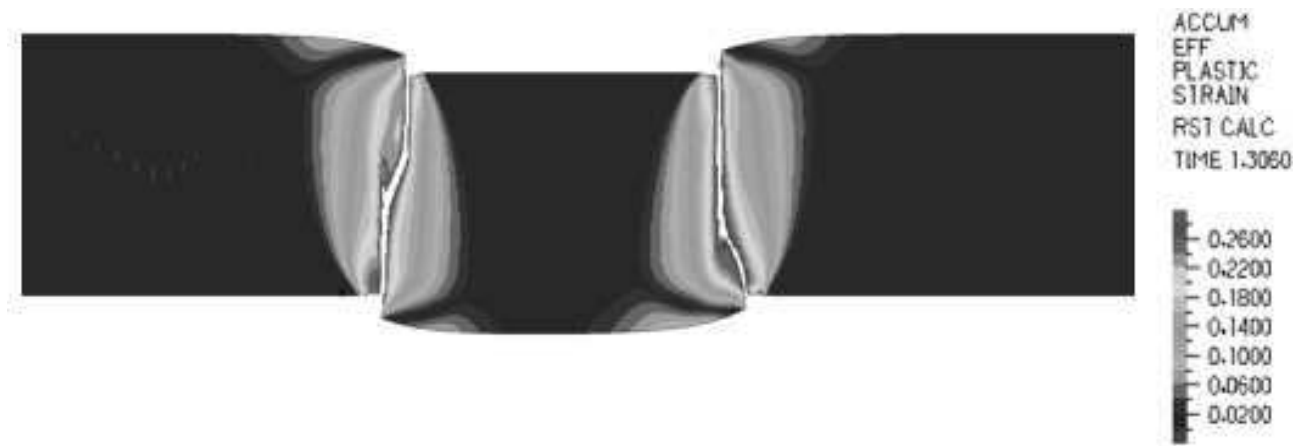


Fig. 5 Accumulated effective plastic strain after full cracking of the material

The reaction force from the punch was used to create dependence between punch displacement and punching force.

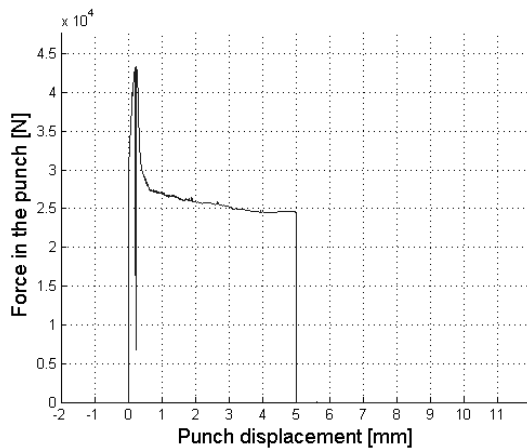


Fig. 6 Blanking force vs. punch displacement

The maximal blanking force obtained by simulation using bilinear elastic-plastic material model was 43396 N.

6 FEM simulation using multi-linear material model

The data obtained from tensile test were used to create

multi-linear elastic-plastic material with isotropic hardening. Young's modulus $E = 210000$ MPa, Poisson's number $\mu = 0.3$. The stress-strain data in true stress representation were used. Rupture of elements occurred at the last stress-strain point. The material model in true stress representation can be seen on the following figure:

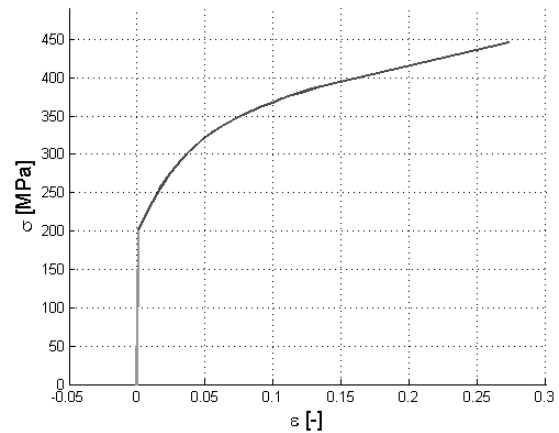


Fig. 7 Stress-strain curve for multi-linear material model in true stress representation

The accumulated effective strain distribution immediately after the material fully cracked can be seen on the following figure.

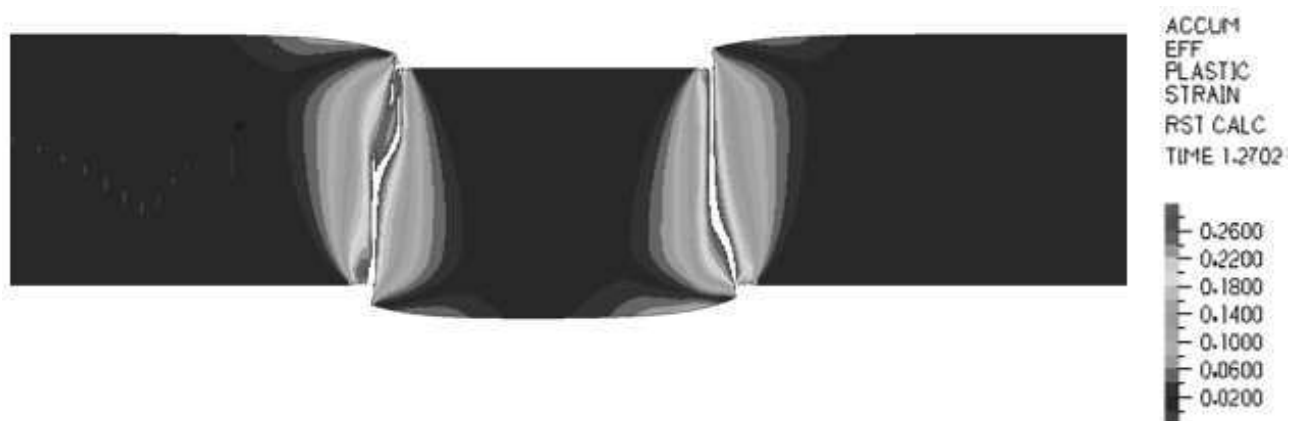


Fig. 8 Accumulated effective plastic strain after full cracking of the material

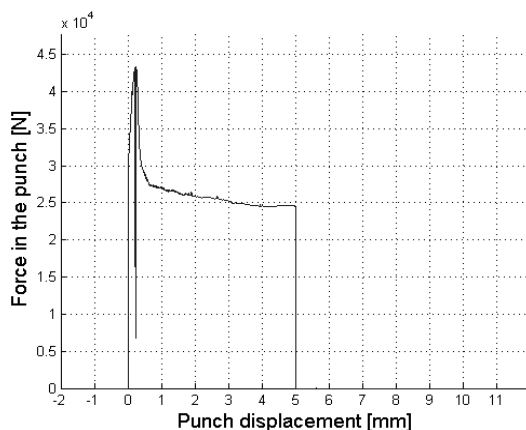


Fig. 9 Blanking force vs. punch displacement

The reaction force from the punch was used to create dependence between punch displacement and punching force.

7 Conclusion

The analytical solution is relatively easy and quick to calculate. The blanking force calculated by analytical solution is 61067 N, blanking force calculated by FEM solution using bilinear elastic-plastic material is 43396 N and blanking force calculated by FEM solution using multi-linear elastic-plastic material is 49921 N. The result of analytical solution is 1.22-1.4 times larger than result of FEM simulation.

Nonlinear finite element solution is much more complex than the presented analytical solution, on the other

hand, the results of FEM solution offer much more than maximal blanking force. The results of FEM simulation also include the shape of resulting surface after blanking. Changing of parameters like clearance between cutting edges of the die and punch during simulation is more cost efficient than using physical prototypes and allows finding of the best parameters for production. FEM simulation can also help to determine the causes of problems which can arise during manufacturing and to find solution to these problems.

Acknowledgement

This work has been supported by grant project KEGA No. 015ŽU-4/2017.

References

- [1] BLATNICKÝ, M., ŠTAUDEROVÁ, M., DIŽO, J. (2017). Numerical Analysis of the Structure Girder for Vehicle Axle Scale Calibration, In: *Procedia Engineering*, 177, pp. 510-515.
- [2] KOPAS, P., JAKUBOVIČOVÁ, L., VAŠKO, M., HANDRIK, M. (2016). Fatigue resistance of reinforcing steel bars, In: *Procedia Engineering*, 136, pp. 193-197.
- [3] ADAMUS, J., LACKI, P., WIECKOWSKI, W. (2011). Numerical simulation of the fine blanking process of sheet titanium, In: *Archives of Metallurgy and Materials*, 56 (2), pp. 431-438.
- [4] HANDRIK, M., VAŠKO, M., KOPAS, P., MÓZER, V. (2016). The linear and nonlinear stability loss of structures due to thermal load, In: *Procedia Engineering*, 136, pp. 359-364.
- [5] NOVAK, P., DEKYS, V. (2015). Induction heating of inner rolling bearing ring in ANSYS, In: *Manufacturing Technology*, Vol. 15, No. 5, pp. 881-885.
- [6] ŽMINDÁK, M., NOVÁK, P., DEKÝŠ, V. (2017). Analysis of bond behaviour in strengthened reinforced concrete beam with carbon fiber reinforced polymer lamella, In: *MATEC Web of Conferences*, 107, art. no. 00045, .
- [7] SAPIETA, M., SAPIETOVA, A., DEKYS, V. (2017). Comparison of the thermoelastic phenomenon expressions in stainless steels during cyclic loading, In: *Metallurgija*, 56 (1-2), pp. 203-206.
- [8] SVOBODA, M., SOUKUP, J. (2013). Dynamic Measurement of Four-Axle Railway Wagon. In: *Manufacturing Technology*, Vol. 13, No. 4 pp. 552-558.
- [9] SVOBODA, M., SOUKUP, J. (2013). Verification of Numeric Solution by Experiment for Examination Vertical Oscillation of a Mechanical System. In: *Manufacturing Technology*, Vol. 13, No. 4, pp. 559-563.
- [10] BITTNER, V., TUČEK, R., PANSKÁ, Š., SVOBODA, M., JELEN K. (2017). Using the Fourier Transform in the Analysis of Vibration Load Tests of Heterogeneous Mechanical Systems. In: *Manufacturing Technology*, Vol 17, No. 6, pp. 839-841.
- [11] ASTARITA, A., PRISCO, U. (2017). Tensile Properties of a Hot Stretch Formed Ti-6Al-4V Alloy Component for Aerospace Applications. In: *Manufacturing Technology*, Vol. 17, No. 2, pp. 141-147.
- [12] KOVÁCS, G. (2016). Productivity Improvement of Assembly Lines by Lean Methods. In: *Manufacturing Technology*, Vol. 17, No. 2, pp. 192-197.